Earth and Planetary Science Letters 283 (2009) 111–121

Contents lists available at ScienceDirect

Earth and Planetary Science Letters

journal homepage: www.elsevier.com/locate/epsl

What controls interplate coupling?: Evidence for abrupt change in coupling across a border between two overlying plates in the NE Japan subduction zone

Naoki Uchida *, Junichi Nakajima, Akira Hasegawa, Toru Matsuzawa

Research Center for Prediction of Earthquakes and Volcanic Eruptions, Tohoku University, Aramaki Aza Aoba, Aoba-ku, Sendai 980-8578, Japan

ARTICLE INFO

Article history:
Received 15 January 2009
Received in revised form 27 March 2009
Accepted 3 April 2009
Available online 13 May 2009

Editor: R.D. van der Hilst

Keywords:
interplate coupling
small repeating earthquake
northeastern Japan subduction zone
Philippine Sea plate
quasi-static slip
Japan trench

ABSTRACT

Interplate coupling in the southernmost extent of the northeast Japan subduction zone (east off-Kanto, Japan) is investigated in detail using a large data set of small repeating earthquakes. In this region of the trench-trench-trench type triple junction, the subducting Pacific plate is in contact with two different overlying plates (the North American and Philippine Sea plates). The border between the two overlying plates extending northwestward from the triple junction is identified along the upper surface of the Pacific plate based on the slip vectors of many interplate events including small repeating earthquakes. The interplate coupling coefficient estimated from the cumulative slip of small repeating earthquakes for the period from 1993 to 2007 reveals a distinct change from south (ca. 0.3) to north (ca. 0.7) across the border. This border also corresponds to the southern limit of the source areas of M>7 interplate earthquakes in the last 80 years along the Japan trench, again indicating the stronger coupling to the north. We also investigate hypocenter distribution and seismic velocity structure along the plate boundary from a large number of travel-time data obtained from the nationwide seismograph network. The results reveal a distinct low-velocity zone just above the Pacific plate and low seismicity along the plate boundary in the region overlain by the Philippine Sea plate, whereas there are no low-velocity zones and the seismicity is high in the region overlain by the North American plate. These observations imply that the geological difference of overlying plate controls large-scale coupling at the plate interface.

1. Introduction

The factors controlling interplate coupling are one of fundamental issues of seismology. In subduction zones, the absolute velocity of the upper plate normal to the trench, the age of subducting plate (e.g. Uyeda and Kanamori, 1979; Peterson and Seno, 1984), thermal condition (e.g. Hyndman and Wang, 1993; Oleskevich et al., 1999) and unconsolidated sediments (e.g. Oleskevich et al., 1999) are pointed out to be the factors controlling interplate coupling. These results are mostly based on global survey of subduction zones, however, recent high-resolution estimation of interplate coupling based on geodetic and recurrent large earthquake data reveal heterogeneous distribution of interplate coupling within a single subduction zone (e.g. Wallace et al., 2004; Yamanaka and Kikuchi, 2004; Suwa et al., 2006; Ohta et al., 2006). Such regional differences in interplate coupling brought us a new phase studying the controlling factor of the interplate coupling.

In the southernmost portion of the northeastern Japan subduction zone (Kanto) three plate boundaries exist as shown in Fig. 1. The Pacific plate (PA) subducts beneath the North American (NA) or Okhotsk plate at the Japan trench in the northern extent of this interaction region, while the Philippine Sea plate (PH) subducts beneath the NA at the Sagami Trough and the PA subducts beneath the PH to the south (e.g. Kasahara, 1985; Ishida, 1992; Matsubara et al., 2005a; Hori, 2006). This means that the plate overlying the PA changes from the NA in the north off Kanto to the PH in the south (Fig. 1b). Seismicity in this area is also somewhat different from that at the northern part of the northeastern (NE) Japan subduction zone: there are dense seismicity and aftershock regions of M>7 interplate earthquakes to the north of ~36 N but there are less seismicity and no M>7 earthquakes to the south of ~36 N (Fig. 2).

Some of recent studies of interplate coupling in regional scale have suggested that the geological terrane or seismic velocity structure of the overlying plate affects the strength of seismic coupling (e.g., Yamamoto et al., 2006; Brudzinski and Allen, 2007; Zhao et al., 2007; Reyners and Eberhart-Phillips, in press). The estimation of interplate coupling across the border of two different overlying plates therefore provides a unique opportunity to test the influence of the overlying plate on interplate coupling.

The interplate coupling at this area itself is also important because the area corresponds to the Tokyo metropolitan area, the locus of about 40% of Japan's economic activities. This area was historically suffered from frequent M~7 earthquakes in addition to M~8 earthquakes with recurrence interval of several hundred years on the Philippine Sea plate

* Corresponding author. Research Center for Prediction of Earthquakes and Volcanic Eruptions, Graduate School of Science, Tohoku University, Aoba-ku, Sendai 980-8578, Japan. Tel.: +81 22 225 1950; fax: +81 22 264 3292.
E-mail address: uchida@aob.geophys.tohoku.ac.jp (N. Uchida).

0012-821X/$ – see front matter © 2009 Elsevier B.V. All rights reserved.
doi:10.1016/j.epsl.2009.04.003

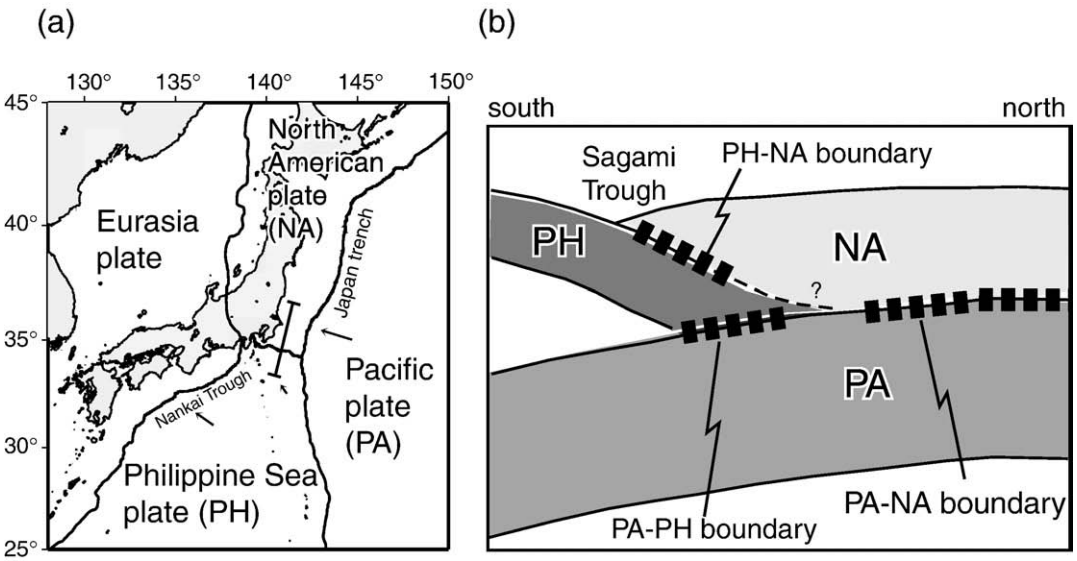

Fig. 1. (a) Tectonic setting around the southernmost extent of the NE Japan subduction zone. (b) Schematic representation of plate configuration east off Kanto along a line shown in (a).

(e.g. the 1703 and 1923 Kanto earthquakes). Although the Japanese government estimated that the possibility of the M7 earthquake in the next 30 years is 70% (Earthquake Research Committee, 2004) from timing of five M~7 earthquakes that occurred after 1885, the source faults for these earthquakes are not well known. Therefore the estimation of interplate coupling will contribute to constrain the unknown source faults.

In this study we focus on the upper boundary of the PA. Our knowledge for the location of the border between the two overlying

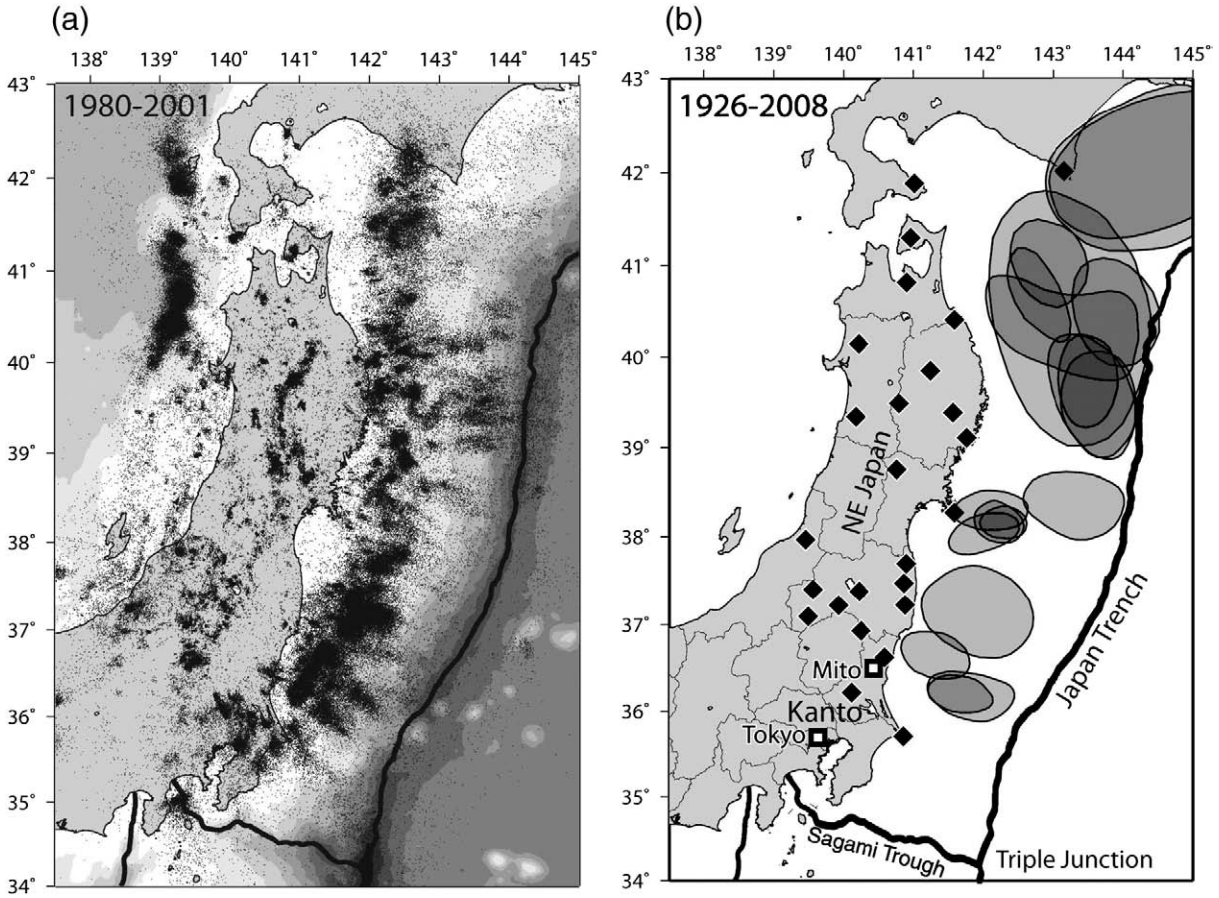

Fig. 2. (a) Epicenter distribution of shallow earthquakes (depth ≤ 60 km) for the period from 1980 to 2001. Seismic catalogue of Tohoku University was used here. (b) Spatial distribution of aftershock areas for earthquakes with M≥7. Aftershock areas for the earthquakes between 1926 and 1983 are from Hasegawa et al. (1985), and the areas for the earthquakes between 1984 and 2008 are estimated in this study. Diamonds are seismic stations used for repeating earthquake analysis.

plates for the PA and spatial distribution of interplate coupling on the PA is, however, insufficient to examine the influence of the overlying plate on interplate coupling in details. This is due to the complexity of the plate geometry in this region and the lack of offshore observations (e.g. Seno and Takano, 1989; Nishimura et al., 2007). To overcome these difficulties, we use a new large dataset of focal mechanisms from broadband waveforms by Full Range Seismograph Network of Japan (F-net) (Broadband Seismic Network Laboratory, National Research Institute for Earth Science and Disaster Prevention, 2008) to constrain the border. Then, we estimate precise interplate coupling distribution across the border from small repeating earthquake data that can estimate offshore interplate slip escaping from the effect of structural complexity (e.g., Ellsworth, 1995; Nadeau and McEvilly, 1999; Igarashi et al., 2003; Uchida et al., 2003).

2. Small repeating earthquakes

Small repeating earthquakes are thought to be caused by the repeated rupture of small asperities (seismic patches) within a stably sliding region of a fault plane. Such repeating earthquakes mostly occur on faults characterized by high deformation rates, such as plate boundaries, and have thus proven particularly useful in delineating plate boundaries (e.g. Kimura et al., 2006) and estimating quasi-static slip rates on plate boundaries (e.g. Ellsworth, 1995; Nadeau and McEvilly, 1999; Igarashi et al., 2003; Uchida et al., 2003, 2004; Nadeau and McEvilly, 2004; Matsubara et al., 2005b; Uchida et al., 2006).

We use waveform similarity to identify the small repeating earthquakes in the southernmost extent of the NE Japan subduction zone (34.5°–38.0°N, 139°–144°E). Digital seismograms recorded by our institute for the period from 1993 to March 2007 are reproduced for analysis from more than 2700 magnet optical disks and hard disk arrays. Seismograms of about 20,000 shallow (depth<95 km) earthquakes with magnitudes 2.5 or larger at seismic stations of the microearthquake observation network of Tohoku University and University of Tokyo (Fig. 2b) are used in the analysis. The sampling frequency is 100 Hz and most of the seismometers were of 1 Hz velocity type.

The coherence of waveforms for all the event pairs with epicentral separations of less than 30 km is calculated following the method of Uchida et al. (2006). The time windows for seismogram analysis are set at 0–40 s from the P-wave arrivals. This time window always contains the S phase, ensuring that events with high coherence have the same S–P times (and hence the same hypocenter locations). An earthquake pair is considered to represent a repeating earthquake pair if the average of coherences at 1, 2, 3, 4, 5, 6, 7, and 8 Hz is larger than 0.95 at two or more stations. A pair (group) of repeaters is linked with another pair (group) if the two pairs (groups) share an earthquake in common.

We identify 1015 small repeating earthquakes with magnitude 2.5 to 4.8 between 1993 and March 2007. A total of 350 groups of repeating earthquakes are identified, each comprising an average of 2.9 events. Fig. 3 shows distribution of small repeating earthquake groups that are presumed to be located on the plate boundary. Groups with various depths (denoted by color) in the offshore area are due to poor depth control because of the absence of near-source stations, while the depth variation in inland and near shore area is due to presence of the two plate boundaries. The inland repeating earthquakes with depths of 20–50 km and 50–90 km are consistent with the locations of the upper boundary of the PH and the upper boundary of the PA (lower boundary of the PH), respectively, according to the plate models of Hirose et al. (2008) and Nakajima and Hasegawa (2006). Thus, the repeating earthquakes are classified into two groups that occurred at the upper surfaces of the PH (diamonds) and the PA (circles) as shown in Fig. 3.

The small repeating earthquakes at the upper surface of the PA, which we will use in the estimation of the border of overlying plates and interplate coupling coefficient, cover most of the area between the Japan trench and costal area of Kanto. The distribution of small repeating earthquakes at the upper surface of the PH is very similar to the result of Kimura et al. (2006, in press), demonstrating the stability of the small repeating earthquake analysis.

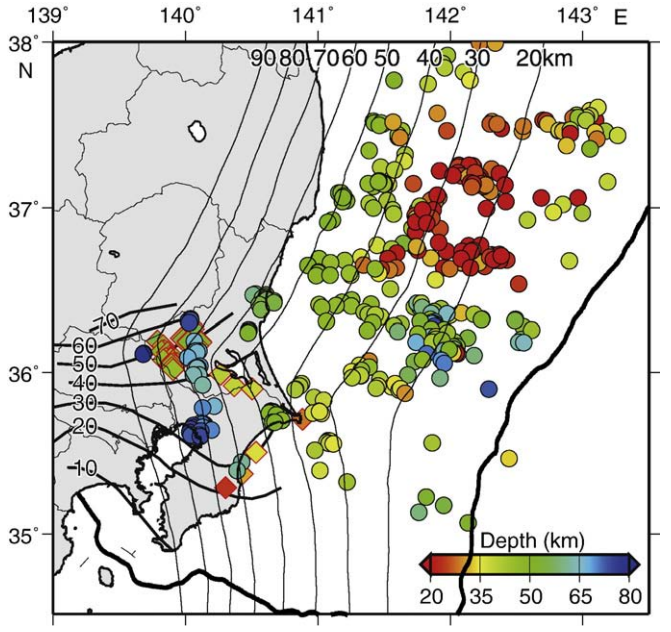

Fig. 3. Locations of small repeating earthquake groups. Circles denote groups on the upper surface of the PA and diamonds denote groups on the upper surface of the PH. The color of symbol shows its focal depth. Thin and bold contours denote the models of the upper surface of PA (this study) and the upper surface of the PH (Hirose et al., 2008), respectively.

3. The border of overlying plates for the Pacific plate

To estimate the border of overlying plates for the PA (northeastern limit of the PH), we use low-angle thrust-fault type earthquakes (depth<90 km; dip<30) in the catalogue of the F-net focal mechanism database for the period between February 1997 and November 2007 in addition to small repeating earthquakes. Here we only use focal mechanisms whose variance reduction is greater than 80% and the number of used stations is greater than three to ensure the quality. Because these earthquakes are thought to be interplate earthquakes between PA, PH and NA and the slip vectors of the earthquakes should be consistent with relative plate motions between these plates, we examine the distribution of slip vectors for these earthquakes.

The slip vectors of small repeating earthquakes (bold vectors) and low-angle thrust-fault type earthquakes (thin arrows) are shown in Fig. 4. They are classified into PA–PH type (red arrows), PA–NA type (blue arrows) and PH–NA type (green arrows) according to slip direction. The three categories (Fig. 4b) are consistent with the relative motions between the plates expected from global plate models (Seno et al., 1993; DeMets et al., 1994; Sella et al., 2002). Here, we use the Okhotsk plate instead of the NA plate when calculating relative plate motions by Sella et al. (2002) because they assume that the Kanto district belongs to the Okhotsk plate.

A distinct northeastern limit can be recognized for the area in which slip vectors of interplate events indicate the presence of the PH (Fig. 4a). Note that both the PH–NA type and PA–PH type slip vectors indicate the presence of the PH. With few exceptions, the angular distributions of the slip vectors in regions I and II (Fig. 4a) indicate a significant difference in slip angle across this border between the overlying PH and NA. This border can therefore be regarded as the

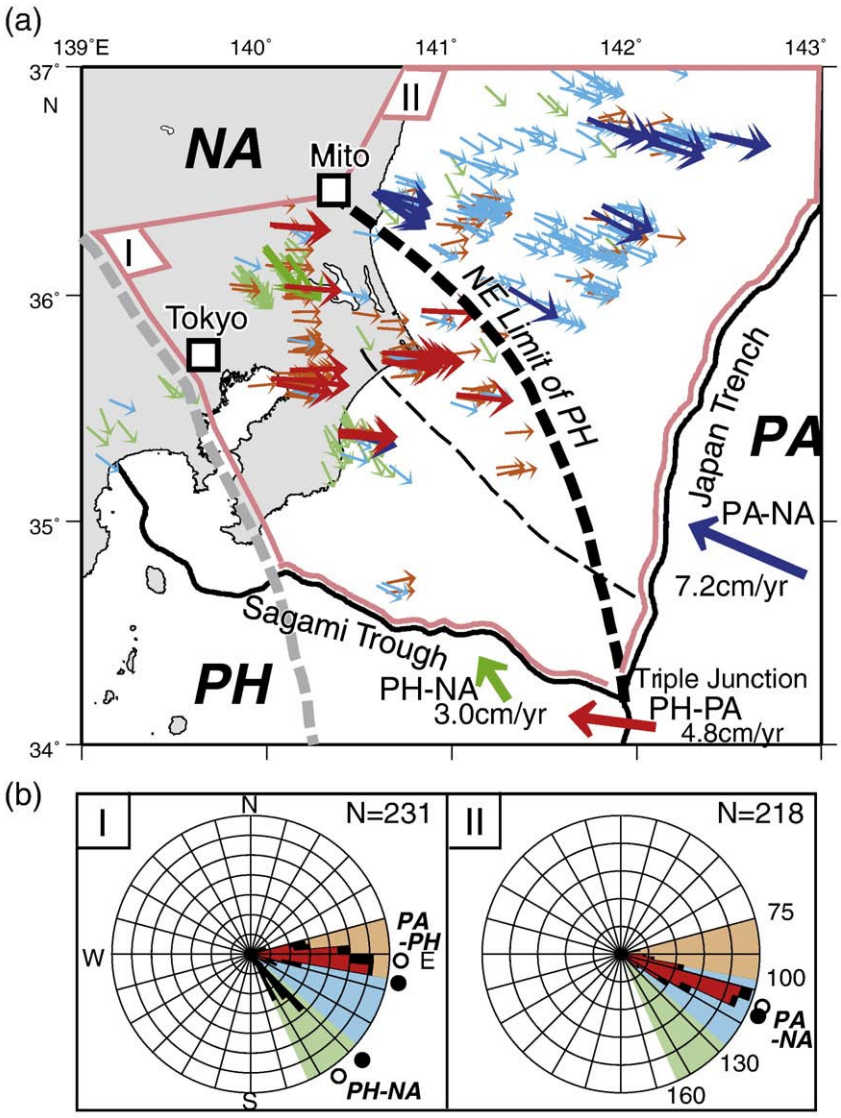

Fig. 4. (a) Slip vectors of small repeating earthquakes on the PA (bold arrows) and other low-angle thrust-fault type earthquakes (thin arrows). Slip vectors are color-coded according to orientational groups of 75–100° (red, orange), 100–130° (blue, cyan), and 130–160° (green). Bold and thin dashed lines denote the northeastern limit of the PH according to this study and Seno and Takano (1989), respectively. Dashed gray line denotes the southwestern limit of PH–PA contact zone (Nakajima et al., 2008). (b) Frequency distribution of slip vectors in regions I (PH–PA contact zone) and II (NA–PA contact zone). Black and red denote all earthquakes and the earthquakes located within 10 km of the upper surface of the Pacific plate (see Fig. 3), respectively. White and black dots denote slip directions expected from the REVEL 2000 (Sella et al., 2002) and NUVEL-1A (Seno et al., 1993; DeMets et al., 1994) plate models, respectively.

northeastern limit of the PH at depth, or the border between the two plates overlying the PA.

To ensure this result, we investigate the slip vectors of earthquakes along the upper surface of the PA, which we modeled by updating the one proposed by Nakajima and Hasegawa (2006) based on the depths of small repeating earthquakes (Fig. 3). We select events located within 10 km of the upper surface and regard them as the events at the surface. The histogram of slip angles for the events (red bars in rose diagram of Fig. 4b) show clear difference between region I and region II.

4. Change in interplate coupling across the border of overlying plates

To estimate interplate coupling on the PA, we first estimate spatial distribution of the interplate slip rate by using the cumulative slip of small repeating earthquakes. Because the small repeating earthquakes slip at the same location (on a small asperity), the cumulative slip reveals the slip history for a given small asperity. An empirical relationship between seismic moment (M_0) and slip (d) proposed by Nadeau and Johnson (1998) is employed to estimate the cumulative slip, as given by

$$log(d) = -2.36 + 0.17log(M_0), \quad (1)$$

where d is given in cm and M_0 is in dyne cm.

This relationship is the same as that used by Igarashi et al. (2003) and Uchida et al. (2003) to investigate the slip rate distribution on the plate boundary east of the northeastern Japan arc based on small repeating earthquake data. The scalar moment for each event is estimated from the magnitude determined by the Japan Metrological Agency using the relationship between magnitude and scalar moment (Hanks and Kanamori, 1979). The slip rate is estimated from cumulative slip of each small repeating earthquake group and time length of the data analysis.

The spatial distribution of interplate slip rate for the period from 1995 to March 2007 is shown in Fig. 5a. We estimate averaged slip rates from small repeating earthquake sequences (black dots) within a

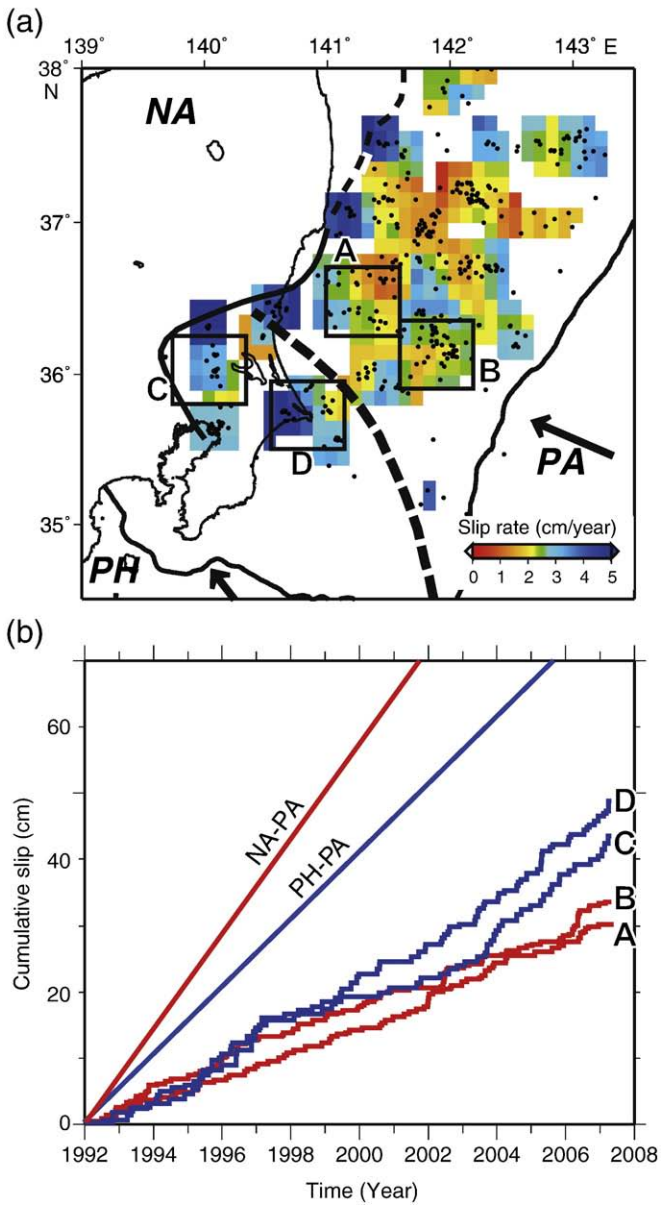

Fig. 5. (a) Spatial distribution of slip rate (color) for the period from 1992–2007. Averaged slip rate is estimated from small repeating earthquake groups within a moving spatial window of 0.3°×0.3° and indicated by a color patch of 0.1°×0.1° at the center of the window. The spatial window is incremented by 0.1°. Black dots denote locations of small repeating earthquake groups and dashed line off Kanto is the same as in Fig. 4. North-south trending solid and dashed black lines denote down-dip limit of interplate earthquakes estimated in this study and determined by Igarashi et al. (2001), respectively. (b) Cumulative slip of small repeating earthquakes averaged over each region labelled A to D. Straight lines denote plate convergence rates for NA–PA and PH–PA boundaries (Sella et al., 2002).

moving spatial window of 0.3 by 0.3°. Here, the estimation is performed for the windows having three or more repeating earthquake groups.

The result shows that the slip rate is relatively large to the south of the border of the overlying plates (Fig. 5a). The feature is also seen in the averaged cumulative slip of small repeating earthquakes in regions A to D (Fig. 5b). The slip amounts are much smaller than those expected from plate model (red and blue lines in Fig. 5b) but the discrepancy is smaller for regions C and D that are located to the south of the border. The other feature is that the areas near the downdip limit of interplate earthquakes estimated by Igarashi et al. (2001) and in this study (dashed and bold lines in Fig. 5a) show faster slip rates than shallower areas. This feature was also observed in the middle part of the NE Japan subduction zone and considered to be due to plate-boundary decoupling at deeper extension of the area (Uchida et al., 2003).

Using the plate convergence rate (v_0) and the slip rate (v), the coupling coefficient (c) in this region is calculated as follows:

$$c = (v_0 - v) / v_0 \quad (2)$$

A coupling coefficient of zero indicates that the fault is creeping at its long-term rate, whereas a coupling coefficient of 1 indicates that the fault is fully locked and is thus building strain to be released in future earthquakes or episodic creep. The plate convergence rates (v_0) are set to be 5.1 cm/yr to the south of the border between the PA and PH, and 7.2 cm/yr to the north of the border between PA and NA (Sella et al., 2002). We estimate interplate coupling coefficient for the location of each small repeating earthquake group and average the coupling coefficients thus obtained by the same way as the slip rate.

The spatial distribution of the interplate-coupling coefficient from Eq. (2) is shown in Fig. 6. The coupling coefficient to the south of the border is low as a consequence of high slip rate and low interplate convergence rate, while that to the north is relatively high as a consequence of the low slip rate and high interplate convergence rate. This result is not affected by the choice of plate model, since most plate models indicate a faster convergence rate in the NA–PA boundary than in the PH–PA boundary, and the estimated slip rate is higher in most locations to the south of the border than to the north of the border (Fig. 5a).

5. Change in interplate seismicity across the border of overlying plates

We relocate earthquakes including the small repeating earthquakes along the upper surface of the Pacific plate to examine the effect of the overlying plates. Earthquakes whose locations are within 10 km in depth from the upper surface were selected for the analysis.

The double difference (DD) hypocenter determination method of Waldhauser and Ellsworth (2000) is applied to the arrival time data of

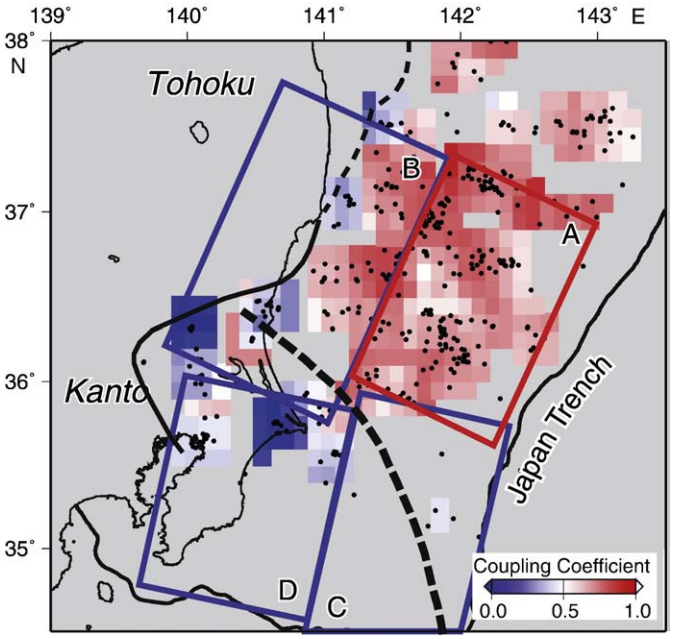

Fig. 6. Spatial distribution of interplate coupling (color) for the same windows shown in Fig. 5. Rectangles indicate sub-faults used in Nishimura et al. (2007) for modeling plate coupling from GPS and leveling data (color denotes coupling coefficient). Bold dashed line and black dots are the same as those in Fig. 5.

the earthquakes obtained by the nationwide seismic network of Japan for the period from 2003 to 2007 (diamonds in Fig. 7). We use a P- and S-wave velocity structure model used in the routine hypocenter determination at Tohoku University (Hasegawa et al., 1978). Event pairs with less than 17 km event separation and having more than 12 arrival time differences for stations with epicentral distances less than 250 km are used for the analysis. A total of 3,074,496 arrival time differences for P-waves, and 2,427,803 for S-waves are used to relocate 23,687 events including 207 small repeating earthquakes. By the relocation the root-mean-square residual of DD data is reduced from 0.1806 s to 0.1074 s.

The relocation result for the earthquakes shows the border of the overlying plates corresponds to the southern limit of intense seismicity along the plate boundary (Fig. 7): in the region where plate boundary is shallower than the down-dip limit of the interplate earthquakes (bold and bold dashed lines), there are continuous dense seismicity to the north of the border (the region surrounded by a blue line in Fig. 7), while the seismicity is sparse to the south of the border. The distribution of large earthquakes (M≥7) in the last 80 years (Fig. 7) is also limited to the north of the border.

We also note that there is heterogeneous distribution of earthquakes even within the low seismicity area to the south of the border. The seismicity is relatively high near the border where the crust part of the PH slab is considered to be in contact with the PA and the seismicity is extremely low for further south region where the mantle part of the PH is thought to be in contact with the PA.

6. Change in seismic velocity structure across the border of overlying plates

We examine seismic velocity structure to investigate the cause of coupling and seismicity change across the border. We use arrival-time data of earthquakes obtained by the nationwide seismic network of Japan for the period from January 2001 to July 2007 (Fig. 8). We select 4783 earthquakes (Fig. 8) with more than 20 arrival-time data to obtain their distribution as uniform as possible. Manually picked arrival times of these earthquakes amount to 403,176 P- and 256,876 S-wave arrival times, which are used for the inversion. Phase picking accuracy is 0.05–0.1 s and 0.1–0.2 s for P- and S-wave arrivals, respectively.

We apply the tomographic inversion method of Zhao et al. (1992a) to determine the 3D P- and S-wave velocity structures. We adopt Japan Meteorological Agency's velocity structure (Ueno et al., 2002) as the initial model for the P-wave velocity structure and constant Vp/Vs value of 1.73 is used to calculate the initial S-wave velocity model. The crustal discontinuities (the Conrad and Moho (Zhao et al., 1992b)) and the upper surface of the subducting PA (Nakajima and Hasegawa, 2006) are adopted in the inversion. In the initial model we assign P-

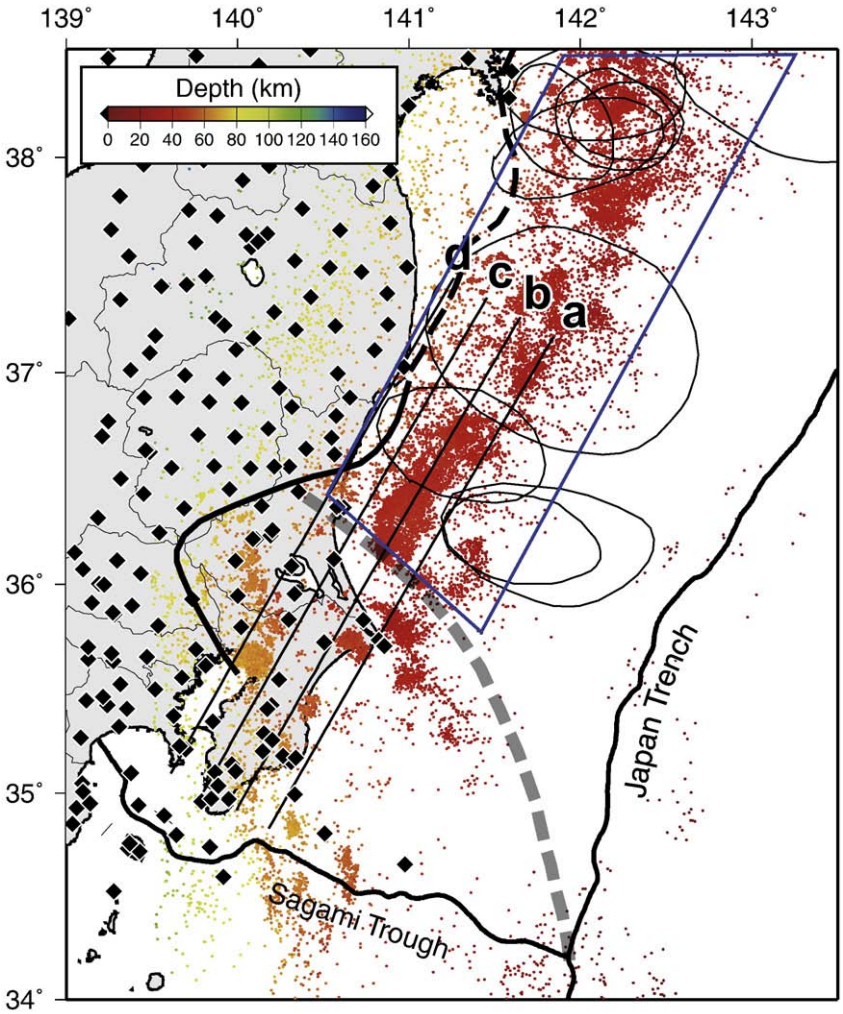

Fig. 7. Epicenter distribution of relocated earthquakes (M≥1) from 2003 to 2007 along the upper boundary of the PA (±10 km from the plate interface model of Nakajima et al. (2008)). The color of the dot shows its focal depth. Outlined aftershock areas are the same as in Fig. 2b. Down-dip limit of interplate events (solid and dashed black lines) and PH–NA border (dashed gray line) are indicated. Black straight lines are locations of cross sections shown in Fig. 9.

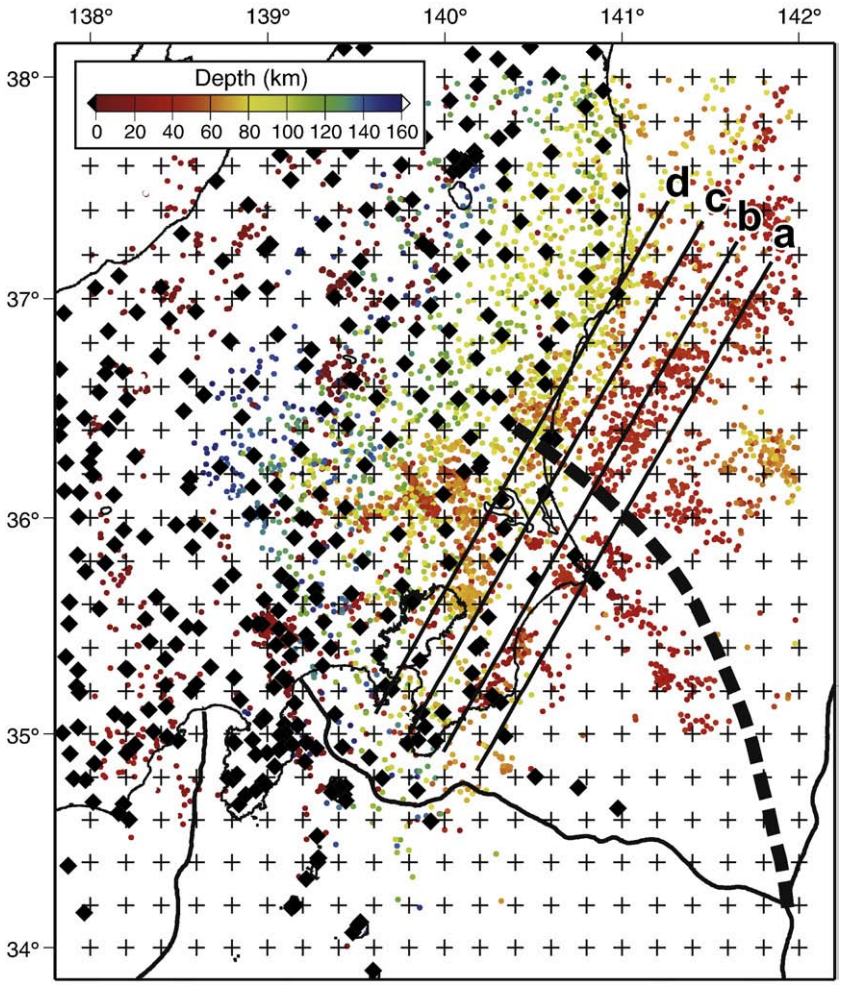

Fig. 8. Earthquakes (dots), stations (diamonds) and grid nodes (crosses) used in the tomographic inversions. The color of dot represents the focal depth of each earthquake. Bold dashed line is the same as that in Fig. 4. Black straight lines show locations of cross sections shown in Fig. 9.

and S-wave velocities within the subducted PA to be 5% faster than those in the surrounding mantle. We set the horizontal grid nodes with a spacing of 0.2° (Fig. 8). Grid nodes are spaced vertically at 5–20 km for depths <160 km and 20–30 km for greater depths.

The final results of seismic tomography are obtained after five iterations and the RMS of residuals for the initial model, which were 0.33 s for the P wave and 0.54 s for the S wave, are reduced to 0.20 s and 0.37 s, respectively, upon optimization. Fig. 9a and b shows P and S wave velocity structure along lines a–d shown in Figs. 7 and 8 together with seismicity along the upper boundary of the PA (the same as the earthquakes in Fig. 7 but relocated by three dimensional velocity model obtained here). The red triangles show the location of the border and solid lines show the plate boundaries.

To ascertain the reliability of the obtained seismic velocity structure, we carry out checkerboard resolution tests by assigning positive and negative perturbations of 6% alternately to the grid nodes both along horizontal and vertical directions. Synthetic data are constructed from the same source-receiver geometry as the observations with random noises corresponding to phase picking errors (a standard deviation of 0.05 s for the P wave and 0.15 s for the S wave). Then we invert the calculated synthetic traveltime data using an initial model.

The result of checkerboard resolution tests are shown on the right of Fig. 9(a) and (b). They show good recovery of assumed velocity perturbations for the areas near the upper surface of the PA. The recovery for the areas far from the boundary is relatively low for offshore region (northern part of lines a and b). The low velocity regions shallower than 30 km and just beneath the plate boundaries are considered to be the crust part of the NA, PH and PA plates. In addition to these low velocity areas, there exists a distinct low velocity zone above the PA in the region overlain by the PH (at the bottom of the PH). It is observed both in P ($Vp \leq 7.2$ km/s) and S wave ($Vs \leq 4.2$ km/s) structures for all cross sections and the Vp/Vs ratio for the low-velocity zone ranges from 1.75 to 1.90. Note that such a low-velocity zone above the PA does not exist in the region overlain by the NA. The small repeating earthquakes (white circles) along the model of the upper surface of the PA ensure the location of the low velocity area is above the upper surface. The seismicity change across the border discussed in the previous section is also prominently seen in cross-section b.

7. Discussion

We summarize the location of the border of overlying plates and its relationship with interplate coupling in the upper surface of the PA in Fig. 10. The border (dashed gray line) extends northwestward from the triple junction to Mito city near the Pacific coast, and it is marked by a change from strong coupling to the north to weak coupling to the south as shown by the distribution of seismic patches (asperities) in Fig. 10c. For the region overlain by the PH, a low velocity zone (red area) was found above the PA (at the bottom of the PH).

The border between the PH and NA plates overlying the PA determined in the present study is located approximately 30 km away to the north from that reported by Seno and Takano (1989) in some

areas (Fig. 4). Although Seno and Takano (1989) employed a similar method, the data set analyzed in their study was approximately 20 times smaller than that examined in the present study. The present result is therefore considered to be more accurate.

The precise distribution of interplate coupling and its change across the border are first discovered in this study. This result seems to be supported by GPS and leveling data analysis by Nishimura et al. (2007). They estimated the coupling coefficients along the plate boundary by back-slip inversions of GPS and leveling data. The results show that the coupling coefficient for faults A and B in Fig. 6 to be 0.8–0.9 and <0.1, respectively. For faults C and D in Fig. 6, they constrained the coupling coefficient to be zero because of limited data resolution but the data indicates that small value is preferable for the region. The inversion results of Nishimura et al. (2007) therefore support the present estimation of the change in coupling across this border of overlying plates. The distribution of M>7 earthquakes along the plate boundary, which are shown in Fig. 2b and Fig. 7 also seems to be consistent with strong coupling to the north of the border.

The border also appears to modulate other characteristics of interplate events. The location of the down-dip limit of interplate events on the PA shown in Fig. 5a, which is estimated from the distribution of repeating earthquakes and other low-angle thrust-type events, shows the limit to the south of the border is anomalously deep (ca. 90 km) compared to that to the north (ca. 50 km). This deepening is probably due to the colder environment at the PA surface which is in contact with the overlying PH (Hasegawa et al., 2007). Small earthquake activity also

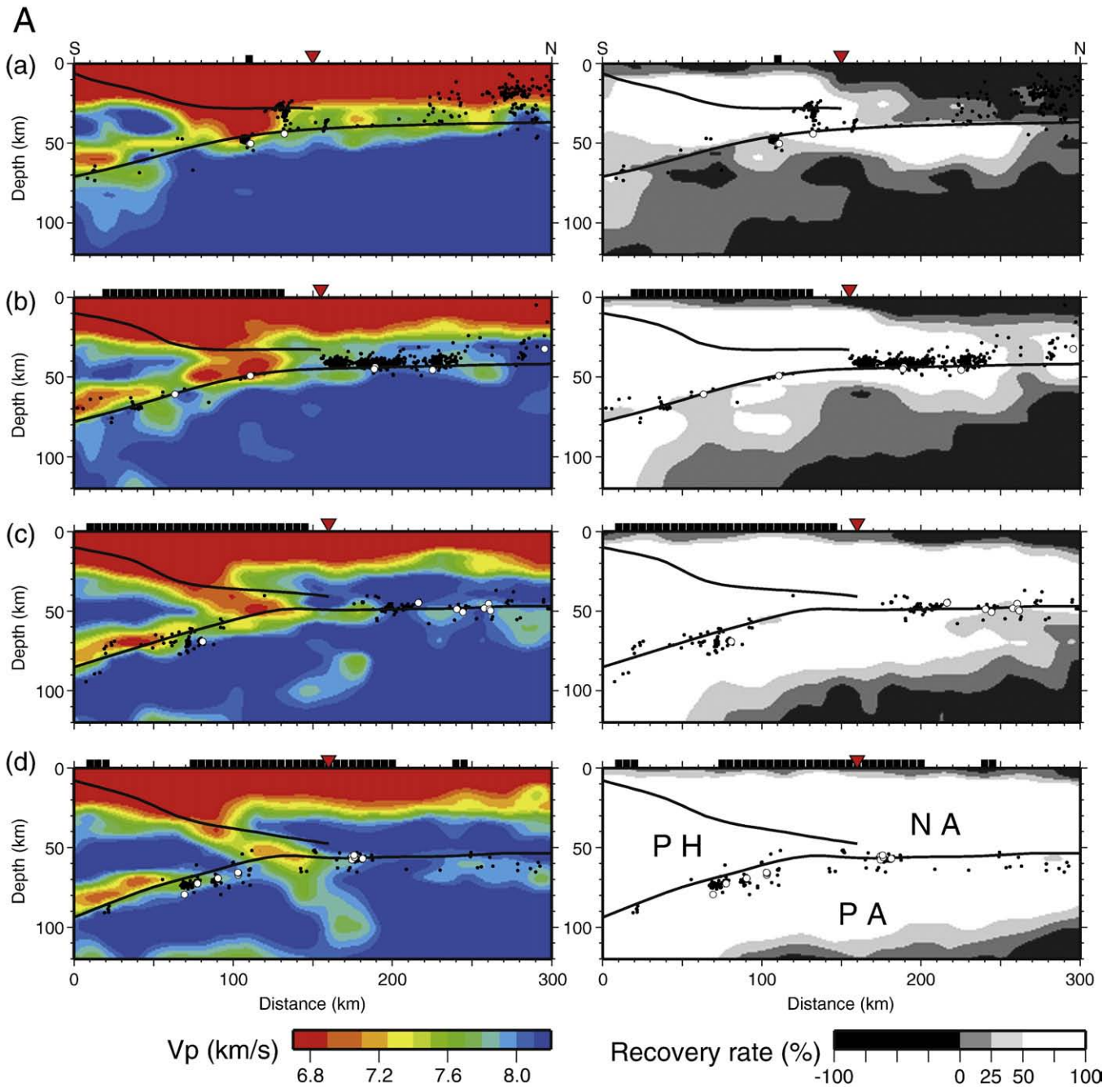

Fig. 9. Vertical cross-sections of seismic velocity structure (left) and recovery rates in the checkerboard resolution tests (right) for P (a) and S (b) waves. Cross-sections along the lines a–d (Figs. 7 and 8) are shown here. White and black points denote small repeating and other earthquakes with magnitude 2 or larger along the upper surface of the PA. Black lines denote the upper surfaces of the PA and PH (Hirose et al., 2008; Nakajima et al., 2008). Red triangle on the top indicates the location of the northeastern limit of the PH (the border of overlying plates for the PA), and bold black line denotes land area.

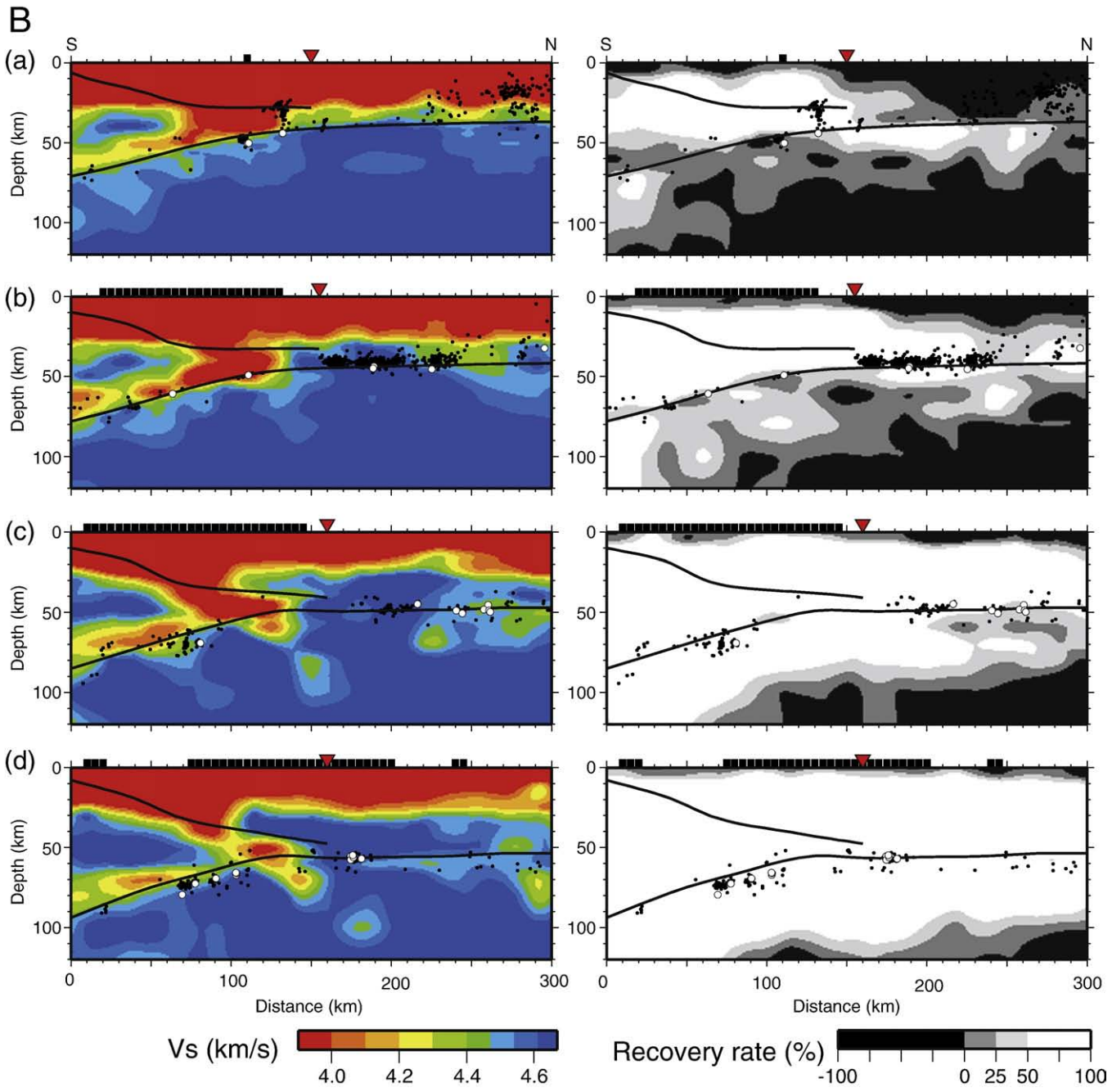

Fig. 9 (*continued*).

appears to be modulated by the change in overlying plate (Fig. 7). The southern limit of intense seismicity to the east of the down-dip limit of interplate events corresponds to the presently identified border as shown in Fig. 7. The vertical cross-section of earthquakes along line b shown in Fig. 9 indicates that most of this concentrated seismicity is considered to be interplate earthquakes on the PA. The area of low seismicity to the south of the border probably reflects decoupling of the plate boundary in most of this area. The weak interplate coupling of the upper boundary of the PA at Kanto estimated in the present study suggests the boundary is not the most likely fault for the M7 earthquakes which are assumed to severely damage the Tokyo metropolitan area.

The features of interplate coupling and seismicity are considered to be related to the change in overlying plate from southwest to northeast. Although there are many factors and models to explain the variety of interplate coupling, the present analysis suggests that interplate coupling is largely controlled by the overlying plate. The underlying plate in the present case is the same across the border, and cannot be assumed to vary in its sediment composition, age, or in the inclusion of seamounts or other large bathymetric features coinciding with the border. High temperature (e.g., Hyndman and Wang, 1993) is not the cause of weak coupling to the south either because the plate boundary between the PH and PA is thought to be relatively cold as discussed above.

The results of seismic tomography reveal a distinct low-velocity zone above the PA in the region overlain by the PH (to the left of the border in Fig. 9), whereas there is no low-velocity zone above the PA in the region overlain by the NA. This suggests that the low velocity material is related to the weak coupling at the area. Low velocity material with similar P wave velocity in the PH mantle above the PA has been found by a reflection/refraction survey along the Izu–Bonin

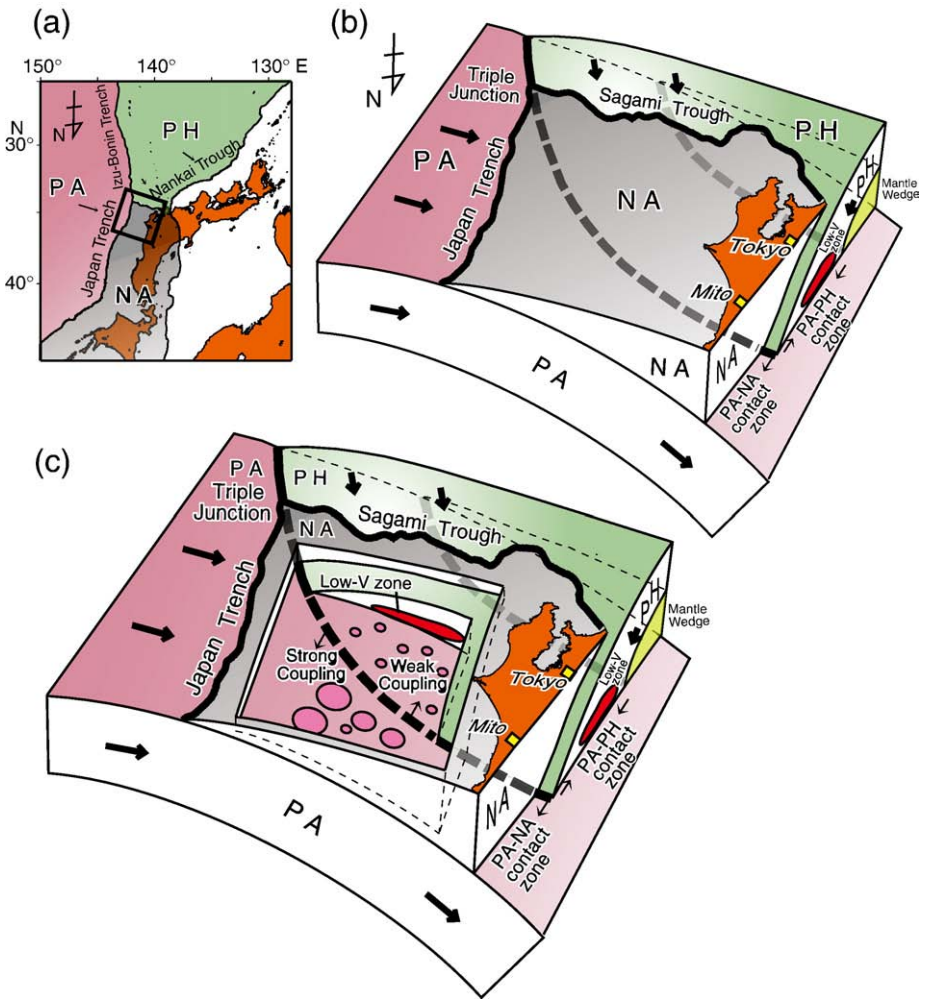

Fig. 10. Schematic figures showing plate configuration and interplate coupling at the upper surface of the PA. (a) Location of schematic figure. (b) Plate configuration of PA, PH and NA. Dashed dark gray and gray lines denote the border of the overlying plates and the downdip limit of the PH–PA contact zone. Red area shows the low velocity area in the lowermost portion of the PH. (c) Difference in interplate coupling across the border of the overlying plates. Large and small patches denote asperities that are responsible for interplate earthquakes.

subduction zone to the south of the present study area (Kamimura et al., 2002). They interpreted the low velocity material as serpentinized peridotite and regarded it as the cause of the weak interplate coupling along the Izu–Bonin trench. Seno (2005) also suggests the serpentinization of mantle wedge as the weak coupling for the area. Considering the fact that the Philippine Sea plate comes from this area and is now subducting beneath Kanto, the low-velocity zone found in the present study can be the same material. The high Vp/Vs ratio (1.75–1.90) for the low-velocity zone, which is often considered as a physical properties of serpentinized peridotite (e.g. Christensen, 1972; Matsubara et al., 2005a), also supports the idea.

8. Conclusions

The border between the two plates, the Philippine Sea and North American plates, overlying the Pacific plate near the triple junction in the northeastern Japan subduction zone is estimated from the slip vectors of interplate events. To the north and south of the border, different seismological features including interplate coupling are apparent. The northern region exhibits strong interplate coupling with a large number of M>7 earthquakes and frequent interplate seismicity, whereas the southern region displays weaker interplate coupling with no M>7 earthquakes in the last 80 years and less frequent interplate seismicity. The geological differences between the two overlying plates are considered to be responsible for the differences in interplate coupling across the border between the Philippine Sea and North American plates overlying the Pacific plate in this area.

Acknowledgements

We used waveforms from seismic networks of the University of Tokyo in addition to the data from Tohoku University. Arrival time data for seismic tomography are provided from Japan Metrological Agency and focal mechanism data are provided from National Research Institute for Earth Science and Disaster Prevention. The authors thank two anonymous reviewers and Editor R. D. van der Hilst for their thoughtful reviews of the manuscript. We also thank F. Hirose, Y. Ito, and T. Iinuma for valuable discussions. This work was supported in part by the Global Center of Excellence (GCOE) program 'Global Education and Research Center for Earth and Planetary Dynamics' at Tohoku University.

References

Broadband Seismic Network Laboratory, National Research Institute for Earth Science and Disaster Prevention, 2008. (http://www.fnet.bosai.go.jp/freesia/index.html).
Brudzinski, M.R., Allen, R.M., 2007. Segmentation in episodic tremor and slip all along Cascadia. Geology 35 (10), 907–910.
Christensen, N.I., 1972. The abundance of serpentinites in the oceanic crust. J. Geol. 80, 709–719.
DeMets, C., Gordon, R., Argus, D., Stein, S., 1994. Effect of recent revisions to the geomagnetic reversal time scale on estimates of current plate motions. Geophys. Res. Lett. 21 (20), 2191–2194.

Earthquake Research Committee, 2004. Long-term Evaluation of Earthquakes along the Sagami Trough. (http://www.jishin.go.jp/main/chousa/04aug_sagami/index.htm).
Ellsworth, W.L., 1995. Characteristic earthquake and long-term earthquake forecasts: implications of central California seismicity. In: Cheng, F.Y., Sheu, M.S. (Eds.), Urban Disaster Mitigation: The Role of Science and Technology. Elsevier, Oxford.
Hanks, T.C., Kanamori, H., 1979. A moment magnitude scale. J. Geophys. Res. 84, 2348–2350.
Hasegawa, A., Umino, N., Takagi, A., 1978. Double-planed structure of the deep seismic zone in the northern Japan arc. Tectonophysics 47, 43–58.
Hasegawa, A., Umino, N., Takagi, A., 1985. Seismicity in the Northeastern Japan arc and seismicity pattern before large earthquakes. Earthq. Predict. Res. 3, 607–626.
Hasegawa, A., Nakajima, J., Kita, S., Okada, T., Matsuzawa, T., Kirby, S., 2007. Anomalous deepening of a belt of intraslab earthquakes in the Pacific slab crust under Kanto, central Japan: possible anomalous thermal shielding, dehydration reactions, and seismicity caused by shallower cold slab material. Geophys. Res. Lett. 34. doi:10.1029/2007GL029616.
Hirose, F., Nakajima, J., Hasegawa, A., 2008. Three-dimensional velocity structure and configuration of the Philippine Sea slab beneath Kanto district, central Japan, estimated by double-difference tomography. J. Seismol. Soc. Jpn., 60 (3), 123–138.
Hori, S., 2006. Seismic activity associated with the subducting motion of the Philippine Sea plate beneath the Kanto district, Japan. Tectonophysics 417, 85–100.
Hyndman, R.D., Wang, K., 1993. Thermal constraints on the zone of major thrust earthquake failure: the Cascadia subduction zone. J. Geophys. Res. 98, 2039–2060.
Igarashi, T., Matsuzawa, T., Umino, N., Hasegawa, A., 2001. Spatial distribution of focal mechanisms for interplate and intraplate earthquake associated with the subducting Pacific plate beneath the northeastern Japan arc: a triple-planed deep seismic zone. J. Geophys. Res. 106, 2177–2191.
Igarashi, T., Matsuzawa, T., Hasegawa, A., 2003. Repeating earthquakes and interplate aseismic slip in the northeastern Japan subduction zone. J. Geophys. Res. 108. doi:10.1029/2002JB001920.
Ishida, M., 1992. Geometry and relative motion of the Philippine Sea plate and Pacific plate beneath the Kanto–Tokai district, Japan. J. Geophys. Res. 97, 453–489.
Kamimura, A., Kasahara, J., Shinohara, M., Hino, R., Shiobara, H., Fujie, G., Kanazawa, T., 2002. Crustal structure study at the Izu–Bonin subduction zone around 31°N: implications of serpentinized materials along the subduction plate boundary. Phys. Earth Planet. Int. 132, 105–129.
Kasahara, K., 1985. Patterns of crustal activity associated with the convergence of three plates in the Kanto–Tokai area, central Japan. Rep. Natl. Res. Cent. Disaster Prev. 35, 33-137.
Kimura, H., Kasahara, K., Igarashi, T., Hirata, N., 2006. Repeating earthquake activities associated with the Philippine Sea plate subduction in the Kanto district, central Japan: a new plate configuration revealed by interplate aseismic slips. Tectonophysics 417 (1), 101–118.
Kimura, H., Kasahara, K., Takeda, T., in press. Subduction process of the Philippine Sea Plate off the Kanto district, central Japan, as revealed by plate structure and repeating earthquakes. Tectonophysics. doi:10.1016/j.tecto.2008.05.012.
Matsubara, M., Hayashi, H., Obara, K., Kasahara, K., 2005a. Low-velocity oceanic crust at the top of the Philippine Sea and Pacific plates beneath the Kanto region, central Japan, imaged by seismic tomography. J. Geophys. Res. 110, B12304. doi:10.1029/2005JB003673.
Matsubara, M., Yagi, Y., Obara, K., 2005b. Plate boundary slip associated with the 2003 Off-Tokachi earthquake based on small repeating earthquake data. Geophys. Res. Lett. 32, L08316. doi:10.1029/2004GL022310.
Nadeau, R.M., Johnson, L.R., 1998. Seismological studies at Parkfield VI: moment release rates and estimates of source parameters for small repeating earthquakes. Bull. Seismol. Soc. Am. 88, 790–814.
Nadeau, R.M., McEvilly, T.V., 1999. Fault slip rates at depth from recurrence intervals of repeating microearthquakes. Science 285, 718–721.
Nadeau, R.M., McEvilly, T.V., 2004. Periodic pulsing of characteristic microearthquakes on the San Andreas fault. Science 303, 220–222.
Nakajima, J., Hasegawa, A., 2006. Anomalous low-velocity zone and linear alignment of seismicity along it in the subducted Pacific slab beneath Kanto, Japan: reactivation of subducted fracture zone? Geophys. Res. Lett. 33, L16309. doi:10.1029/2006GL026773.
Nakajima, J., Hasegawa, A., Hirose, F., 2008. Collision between the Pacific and Philippine Sea slabs and seismotectonics beneath Kanto, central Japan, J248-004, Japan Geoscience Union Meeting 2008, Chiba, Japan, 25–30 May 2008.
Nishimura, T., Sagiya, T., Stein, R.S., 2007. Crustal block kinematics and seismic potential of the northernmost Philippine Sea plate and Izu microplate, central Japan, inferred from GPS and leveling data. J. Geophys. Res. 112, B05414. doi:10.1029/2005JB004102.
Ohta, Y., Freymueller, J.T., Hreinsdottir, S., Suito, H., 2006. A large slow slip event and the depth of the seismogenic zone in the south central Alaska subduction zone. Earth Planet. Sci. Lett. 247 (1–2), 108–116.
Oleskevich, D.A., Hyndman, R.D., Wang, K., 1999. The updip and downdip limits to great subduction earthquakes: thermal and structural models of Cascadia, south Alaska, SW Japan, and Chile. J. Geophys. Res. 104, 14,965–14,991.
Peterson, E.T., Seno, T., 1984. Factors affecting seismic moment release rates in subduction zones. J. Geophys. Res. 89, 10,233–10,248.
Reyners, M., Eberhart-Phillips, D., 2009. Small earthquakes provide insight into plate coupling and fluid distribution in the Hikurangi subduction zone, New Zealand. Earth Planet. Sci. Lett. 282, 299–305. doi:10.1016/j.epsl.2009.03.034.
Sella, G.F., Dixon, T.H., Mao, A., 2002. REVEL: a model for recent plate velocities from space geodesy. J. Geophys. Res. 107 (B4), 2081. doi:10.1029/2000JB000033.
Seno, T., 2005. Variation of downdip limit of the seismogenic zone near the Japanese islands: implications for the serpentinization mechanism of the forearc mantle wedge. Earth Planet. Sci. Lett. 231, 249–262.
Seno, T., Takano, T., 1989. Seismotectonics at the Trench-Trench-Trench triple junction off central Honshu. Pure Appl. Geophys. 129, 27–40.
Seno, T., Stein, S., Gripp, A.E., 1993. A model for the motion of the Philippine Sea plate consistent with NUVEL-1 and geological data. J. Geophys. Res. 98, 17,941–17,948.
Suwa, Y., Miura, S., Hasegawa, A., Sato, T., Tachibana, K., 2006. Interplate coupling beneath NE Japan inferred from three-dimensional displacement field. J. Geophys. Res. 111 101029/2004JB003203.
Uchida, N., Matsuzawa, T., Igarashi, T., Hasegawa, A., 2003. Interplate quasi-static slip off Sanriku, NE Japan, estimated from repeating earthquakes. Geophys. Res. Lett. 30 (15), 1801. doi:10.1029/2003GL017452.
Uchida, N., Hasegawa, A., Matsuzawa, T., Igarashi, T., 2004. Pre- and post-seismic slip on the plate boundary off Sanriku, NE Japan associated with three interplate earthquakes as estimated from small repeating earthquake data. Tectonophysics 385, 1–15.
Uchida, N., Matsuzawa, T., Hirahara, S., Hasegawa, A., 2006. Small repeating earthquakes and interplate creep around the 2005 Miyagi-oki earthquake (M7.2). Earth Planets Space 58, 1577–1580.
Ueno, H., Hatakeyama, S., Aketagawa, T., Funasaki, J., Hamada, N., 2002. Improvement of hypocenter determination procedures in the Japan Meteorological Agency. Q. J. Seism. 65, 123–134 (in Japanese).
Uyeda, S., Kanamori, H., 1979. Back arc opening and the mode of subduction. J. Geophys. Res. 84, 1,049–1,061.
Waldhauser, F., Ellsworth, W.L., 2000. A double-difference earthquake location algorithm: method and application to the Northern Hayward fault, California. Bull. Seismol. Soc. Am. 90, 1353–1368.
Wallace, L.M., Beavan, J., McCaffrey, R., Darby, D., 2004. Subduction zone coupling and tectonic block rotations in the North Island, New Zealand. J. Geophys. Res. 109, B12406. doi:10.1029/2004JB003241.
Yamamoto, Y., Hino, R., Nishino, M., Yamada, T., Kanazawa, T., Hashimoto, T., Aoki, G., 2006. Three-dimensional seismic velocity structure around the focal area of the 1978 Miyagi-Oki earthquake. Geophys. Res. Lett. 33, L10308. doi:10.1029/2005GL025619.
Yamanaka, Y., Kikuchi, M., 2004. Asperity map along the subduction zone in northeastern Japan inferred from regional seismic data. J. Geophys. Res. 109. doi:10.1029/2003JB002683.
Zhao, D., Hasegawa, A., Horiuchi, S., 1992a. Tomographic imaging of P and S wave velocity structure beneath northeastern Japan. J. Geophys. Res. 97, 19909–19928.
Zhao, D., Horiuchi, S., Hasegawa, A., 1992b. Seismic velocity structure of the crust beneath the Japan Islands. Tectonophysics 212, 289–301.
Zhao, D., Wang, Z., Umino, N., Hasegawa, A., 2007. Tomographic imaging outside a seismic network: application to the northeast Japan arc. Bull. Seismol. Soc. Am. 97, 1121–1132.